

# BAYESIAN MULTICHANNEL TRACKING OF A PERIODIC SIGNAL

Thorkild Find Pedersen\*

Brüel & Kjær Sound & Vibration A/S  
Skodsborgvej 307  
DK-2850 Nærum, Denmark  
tfpedersen@bksv.com

Lars Kai Hansen

Informatics and Mathematical Modelling  
Technical University of Denmark  
Richard Petersens Plads, Building 321  
DK-2800 Kongens Lyngby, Denmark  
lkhansen@imm.dtu.dk

## ABSTRACT

The problem of estimating and tracking the fundamental frequency of a periodic signal is formulated in Bayesian terms and a solution is proposed. For multichannel measurements both simulated and experimental data show that the estimate improves when more data channels are used for the estimation. The method is tested on a multichannel vibration measurement from the interior of a passenger car. From the measurements the running speed of the engine is successfully estimated during a run-up/down experiment.

## 1. INTRODUCTION

When analyzing the behaviour of rotating machines, e.g. the vibrations caused by the engine in a passenger car, it is important to know the running speed, or fundamental frequency, of the engine. The fundamental frequency is typically measured using dedicated sensors like proximity probes or photosensors which require direct access to the rotating part of the machine. Rotating parts are often not easy accessible. It is therefore of interest to investigate the possibility of extracting the fundamental frequency from other sources, e.g. the vibration signals being analyzed.

In section 2 Bayesian spectral estimation theory [1, 2] is reviewed in the light of estimating the posterior probability of the fundamental frequency,  $\omega_F$ , conditioned on the measured data, i.e.  $p(\omega_F | D_i, I_k)$  where  $I_k$  symbolizes the prior knowledge in the estimation model, and  $D_i$  represent one or more of the measured signals. Only a fixed model is considered here, but within the Bayesian framework it expandable to multiple models.

By segmenting the source signals into overlapping time records and introducing a prior on  $\omega_F$  conditioned on the previous two records, the estimator is extended to include tracking, i.e.  $p(\omega_F(n) | \omega_F(n-1), \omega_F(n-2))$ , where  $n$  is the number of the current record.

\*This work is funded by the Danish Academi of Technical Sciences through the industrial Ph.d fellowship EF-812

The fundamental frequency estimator and tracker is first tested on a simulated mechanical system with one degree of freedom, described in section 3. Then the experimental data described in section 4 are used for validation. The results from both simulated and experimental data are found in section 5 and 6.

## 2. BAYESIAN ESTIMATION AND TRACKING

In the literature [3, 4] the problem of detecting and tracking periodic signals is often defined as estimating the amplitude and phase of limited number of harmonic components, i.e.

$$d(t) = \sum_{k=1}^K (a_k \cos(\omega_k t) + b_k \sin(\omega_k t)) + e(t) \quad (1)$$

$$e(t) \sim \mathcal{N}(0, \sigma^2) \quad (2)$$

The frequencies in the harmonic sequence are defined as orders  $\alpha_k$  of the fundamental frequency,  $\omega_0$ , i.e.  $\omega_k = \alpha_k \omega_0$ . In [4] the asymptotic Cramér Rao Lower bound is derived for this type of harmonic signal:

$$\text{Var}(\hat{\omega}_F) \geq \frac{12}{\text{SNR} \omega_{\text{eff}}^2 N^3} \quad (3)$$

where  $\text{SNR} = \sum_{k=1}^n c_k^2 / (2\sigma_N^2)$ ,  $c_k^2 = a_k^2 + b_k^2$ , and  $\omega_{\text{eff}}^2 = \sum_{k=1}^n k^2 c_k^2 / \sum_{k=1}^n c_k^2$

Writing (1) in vectorized form, it is seen to be a linear model

$$\mathbf{d} = \mathbf{G} \cdot \mathbf{b} + \mathbf{e} \quad (4)$$

where  $\mathbf{d}$  is the observed data,  $\mathbf{G}$  is a matrix containing basis vectors as columns,  $\mathbf{b}$  is the parameter vector and  $\mathbf{e}$  is a noise vector:

$$\begin{aligned} \mathbf{d}_{N \times 1} &= [d_0, d_1, \dots, d_{N-1}]^T \\ \mathbf{e}_{N \times 1} &= [e_0, e_1, \dots, e_{N-1}]^T \\ \mathbf{b}_{2K \times 1} &= [a_1, b_1, \dots, a_K, b_K]^T \\ \mathbf{G}_{N \times 2K} &= [\cos(\Omega_1), \sin(\Omega_1), \dots, \cos(\Omega_K), \sin(\Omega_K)] \\ \Omega_i &= [\omega_i 0, \omega_i 1, \dots, \omega_i (N-1)]^T \end{aligned} \quad (5)$$

The likelihood of the observed data given all parameters and the characteristics of the noise is

$$p(\mathbf{d}|\mathbf{b}, \mathbf{G}, I_K) = (2\pi\sigma^2)^{-N/2} \exp \left\{ -\frac{(\mathbf{d} - \mathbf{G} \cdot \mathbf{b})^\top \cdot (\mathbf{d} - \mathbf{G} \cdot \mathbf{b})}{2\sigma^2} \right\}$$

and the Maximum Likelihood estimate of the parameters,  $\mathbf{b}$ , is

$$\hat{\mathbf{b}} = (\mathbf{G}^\top \mathbf{G})^{-1} \mathbf{G}^\top \cdot \mathbf{d}$$

Since the likelihood expresses the probability of the data given the parameters, Bayes Rule is used to express the probability of the parameters,  $\theta = [\omega_0, \sigma, \mathbf{b}]$ , given the data,  $\mathbf{d}$ , and the model,  $I_K$ :

$$p(\theta|\mathbf{d}, I_K) = \frac{p(\mathbf{d}|\theta, I_K)p(\theta|I_K)}{p(\mathbf{d}|I_K)} \quad (6)$$

Of the parameters in  $\theta$  only  $\omega_F$  is of interest, therefore uninformative prior distributions are assigned to the *nuisance* parameters,  $\sigma$  and  $\mathbf{b}$ :

$$p(\mathbf{b}|I_K) = k_b \quad p(\sigma|I_K) = \frac{k_\sigma}{\sigma} \quad (7)$$

Integrating out the nuisance parameters, the posterior distribution of  $\omega_F$  is [1]

$$p(\omega_F|\mathbf{d}, I_K) \propto \int_0^\infty \int_{\mathbb{R}^{2K}} p(\mathbf{d}|\omega_0, \sigma, \mathbf{b}, I_K) \frac{1}{\sigma} d\mathbf{b} d\sigma \quad (8)$$

$$\propto \frac{(\mathbf{d}^\top \mathbf{d} - \mathbf{f}^\top \mathbf{f})^{-\frac{(N-2K)}{2}}}{\sqrt{\det(\mathbf{G}^\top \mathbf{G})}} \quad (9)$$

where,  $\mathbf{f}$  is the estimated signal based on the maximum likelihood estimate, i.e.

$$\mathbf{f} = \mathbf{G} \cdot \hat{\mathbf{b}} \quad (10)$$

The posterior is recognized as a student t-distribution.

## 2.1. Multichannel Measurements

When a measurement contains multiple data channels,  $D_1, D_2, \dots, D_N$ , then if the data channels are assumed to be independent, i.e.  $p(D_1, D_2, \dots, D_N) = \prod_i^N p(D_i)$ , the measurements can be combined through the joint probability for the fundamental frequency  $\omega_F$  given all the data channels, i.e.

$$p(\omega_F|D_1, D_2, \dots, D_N) \propto \prod_{i=1}^N p(\omega_F|D_i) \quad (11)$$

## 2.2. Tracking

The posterior in (8) is valid for stationary signals only. In order to track  $\omega_F$  the measurement data is segmented into overlapping records of suitable lengths where  $\omega_F$  is close to stationary.

The posterior  $p(\omega_F(n)|D_x(n), I_k)$  is estimated for each data segment (denoted by the segment number,  $n$ ) and the problem of tracking  $\omega_F$  is now solved by adding a *tracking* prior that conditions  $\omega_F(n)$  on e.g. the previous two record, i.e.  $p(\omega_F(n)|\omega_F(n-1), \omega_F(n-2))$ . Assuming the first order derivative of  $\omega_F$  is constant, i.e.

$$\omega_F(n) - \omega_F(n-1) = \omega_F(n-1) - \omega_F(n-2) + \mathcal{N}(0, \sigma_T^2) \quad (12)$$

the tracking prior becomes

$$p(\omega_F(n)|\omega_F(n-1), \omega_F(n-2)) = \frac{1}{\sqrt{2\pi\sigma_T^2}} e^{-\frac{(\omega_F(n) - 2\omega_F(n-1) + \omega_F(n-2))^2}{2\sigma_T^2}} \quad (13)$$

The combined estimation and tracking algorithm is listen in table 2.

## 3. SIMULATION DATA

The vibration signals are here modelled as the forced response of a mechanical system with a single degree of freedom (SDOF). The equation of motion is governed by

$$m \ddot{x}(t) + c \dot{x}(t) + k x(t) = F(t) \quad (14)$$

where  $m$  is the mass,  $c$  is the damping,  $k$  is the spring forcing and  $F$  is the external forcing on the mass. (') and (") indicates single and double differentiation in time.  $x(t)$  is the displacement of the mass. The frequency response for displacement, velocity and acceleration of the system is shown in figure 1 together with the system. The mechanical system is simulated with a digital filter, which can be derived from the Laplace transform of (14) using the bilinear transform. The driving force is a harmonic signal composed of the first three harmonics of the fundamental frequency (15). The amplitude of the harmonic components are inversely proportional to the order of the component.

$$x(t) = A \sum_{n=1}^3 \frac{1}{n} \cos n\Omega(t), \quad \Omega(t) = \int_0^t \omega_F(\tau) d\tau \quad (15)$$

As is shown in figure 2 the relative amplitude of the orders change as  $\omega_F$  changes and the orders pass through the resonance of the system. The top graph shows the profile of the harmonic orders of  $\omega_F$ . The lower graph shows the RMS acceleration amplitudes of the harmonic orders<sup>1</sup>.

<sup>1</sup>The units used have no physical interpretation.

White Gaussian noise with a constant variance,  $\sigma_N^2$ , is added to the simulated response of the mechanical system. The simulated response thus becomes with  $\star$  denoting convolution and  $h_T(t)$  being the impulse response of the system modelled. The noise variance is determined from an overall SNR level defined as  $SNR_{db} = 10 \log(\text{Var}(y)/\sigma_N^2)$ , where  $y$  is the response. Since the effect of  $y(t)$  varies over time, so will the actual SNR level which is also observed in practice. In the simulations the three responses, acceleration, velocity and displacement are used as independent source signals.

#### 4. EXPERIMENTAL DATA

The experimental data consists of three vibration channels and one tacho channel for reference. The vibration signals are measured with a tri-axial accelerometer placed on the mounting bolt of the front seat in a passenger car. The signals are labeled  $D_x$ ,  $D_y$  and  $D_z$ . The tacho channel was connected to an photo-sensitive probe emitting one pulse per revolution on the crankshaft, being equivalent to half the fundamental frequency (it was a 4 stroke engine). All data was recorded with a B&K Pulse multi-analyzer and the digitized data was processed using Matlab. For the purpose of finding  $\omega_F$  the exact scaling of the signals are not of importance, therefore the digitized values of the conditioned analog signals have been used unscaled.

During the measurement the car is in neutral and the running speed is increased in steps; for the first 15 seconds the engine is running approximately 1000 RPM, for the next 25 seconds approx. 2000 RPM, then for 10 seconds 3500 RPM whereafter it drops to idle for the remaining 10 seconds. Figure 5 shows a typical spectrogram of one of the vibration signals. The signal is seen to contain many higher order harmonics of the RPM profile, but no specific order stands-out clearly. In general the signal is very noisy. The vibration signals were sampled at 1024 samples per second, while the tacho signal was sampled at 65536 samples per second and linear interpolation<sup>2</sup> was used to improve the accuracy of the  $\omega_F$  reference.

#### 5. SIMULATION RESULTS

100 Monte Carlo simulations are made of the simulated vibration signals. Each signal is segmented into records of 1/4 second with 75% overlap. In each simulation, the posterior distribution of  $\omega_F$  is computed for the harmonic sequence  $K = [1, 2, 3]$ .

The posteriors of  $\omega_F$  for each signal are computed, and the joint posterior formed. The tracking prior is initialized

<sup>2</sup>Linear interpolation does not give the best accuracy, but sufficient for these comparisons. Better precision is obtained by opsampling the tacho signal and using higher order interpolation schemes [5].

with

$$p(\omega_F(0)) = \mathcal{N}(10, 1), \quad \sigma_T^2 = 1.0$$

for each posterior distribution. The results are summarized in figure 4, where the standard deviation of the  $\omega_F$  estimates are plotted with symbols; with lines are shown the Cramér Rao lower bounds. The simulated results are very close to the CRLB which indicates that the Bayesian tracker is optimal. The tracker was initialized with

#### 6. EXPERIMENTAL RESULTS

Each of vibration signals,  $D_x$ ,  $D_y$ ,  $D_z$  were segmented into records of 1/4 second, overlapping 75%. For each segment the posterior of  $\omega_F$  was computed for the harmonic sequence  $K = [1, 2, 2.5]$ . The three posteriors were then combined. The initial value for the tracker was set to

$$p(\omega_F(0)) = \mathcal{N}(12, 3), \quad \sigma_T^2 = 0.8$$

Figure 7 shows the result of tracking on the individual posterior distributions  $p(\omega_F|D_x)$ ,  $p(\omega_F|D_y)$ ,  $p(\omega_F|D_z)$  and the joint posterior,  $p(\omega_F|D_x, D_y, D_z)$ . It is seen that each of the individual tracks fail at different times:  $D_x$  fails initially to track at 1000 RPM the first 10 seconds;  $D_y$  cannot keep up with the jump from 2000 to 3500 RPM and loses track;  $D_z$  loses track de-accelerating from 3500 RPM and does not return to idle. The tracking error is defined as the difference between the obtained track and the measured tacho reference. Table 1 summarizes the result of tracking on all posterior combinations of the source signals. The table shows the mean error in column 2, the standard deviation  $\sigma$  in column 3 and the maximum absolute error in column 4. The table shows convincingly that the estimate improves as the signals are combined.

#### 7. CONCLUSION

Here the Bayesian paradigm has proven succesful in devising a method to estimate and track the fundamental frequency of a rotating machine from a multichannel vibration measurement.

Starting with the conditioned posterior distribution of  $\omega_F$  given measured data, the model was first extended from a single channel estimation to multichannel estimation via the formulation of the joint probability of the data. Then by introduction of prior distribution for  $\omega_F(t)$  given previous estimates, tracking was readily at hand.

The method was tested on simulated and experimental data with great success. Simulations showed that the estimate meets the Cramér Rao lower bound, and the experimental data showed the methods usefulness in solving the practical problem of determining the running speed of the engine in a passenger car. Not only was the method capable

of providing accurate estimates, but also able to track rapid speed changes.

For the method to be of practical use however, there are some issues to be addressed. Choosing the right tracking variance can be difficult, perhaps this could be solved using the Baum-Welch algorithm. Choosing the most appropriate harmonic sequence for the spectrum estimator is important, the Bayesian paradigm allows the method e.g. to be expanded to operate with multiple harmonic sequences. Furthermore reversible jump MCMC procedures [6] could be investigated for selecting the best harmonic model.

## 8. REFERENCES

- [1] Joseph J.K. Ó Ruanaidh and William J. Fitzgerald, *Numerical Bayesian Methods Applied to Signal Processing*, Statistics and Computing. Springer, 1998.
- [2] G. L. Bretthorst, *Bayesian Spectrum Analysis and Parameter Estimation*, vol. 48 of *Lecture Notes in Statistics*, Springer-Verlag, 1988, Available online: [www.bayes.wustl.edu](http://www.bayes.wustl.edu).
- [3] P.J. Parker and B.D.O. Anderson, "Frequency tracking of nonsinusoidal periodic signals in noise," *Signal Processing*, vol. 20, no. 2, pp. 127–52, 1990.
- [4] A. Nehorai and B. Porat, "Adaptive comb filtering for harmonic signal enhancement," *IEEE Transactions on Acoustics, Speech and Signal Processing*, vol. ASSP-34, no. 5, pp. 1124–38, 1986.
- [5] K. R. Fyfe and E. D. S. Munck, "Analysis of computed order tracking," *Mechanical Systems & Signal Processing*, vol. 11, no. 2, pp. 187–205, 1997.
- [6] C. Andrieu and A. Doucet, "Joint bayesian model selection and estimation of noisy sinusoids via reversible jump mcmc," *Signal Processing, IEEE Transactions on*, vol. 47, no. 10, pp. 2667–2676, 1999.

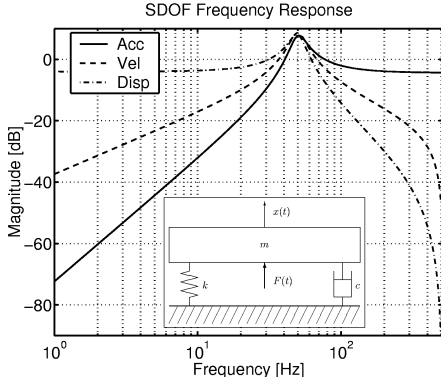


**Fig. 1.** Frequency responses for the second order filter simulating the mechanical system with a single degree of freedom (insert): Acc - acceleration responses; Vel - velocity response and Disp - displacement response.

Data	Mean Error	$\sigma$	Max. Error
$D_x$	-1.3	3.1	9.1
$D_y$	3.3	18	64
$D_z$	0.33	1.7	9.9
$D_{xy}$	0.057	0.6	5.1
$D_{xz}$	0.17	1.6	9.9
$D_{yz}$	0.099	0.77	5.8
$D_{xyz}$	0.059	0.57	5.1

**Table 1.** Tracking Results. From the three source signals a total of 7 posterior distributions can be formed. The result of tracking on each of the combinations are summarized here. For each track the mean tracking error, its standard deviation ( $\sigma$ ) and the maximum absolute error is shown. Significant improvements are observed when the sources are combined.

For each data segment  $n$  do:

- Compute  $p(\omega_F | D_i, I_k)$  for all channels  $i = 1 \dots N$
- Compute joint posterior,  $p(\omega_F | D_1, \dots, D_N, I_k)$
- $\hat{\omega}_F(n) = \max_{\omega_F} p(\omega_F | D_1, \dots, D_N, I_k) p(\omega_F | \hat{\omega}_F(n-1), \hat{\omega}_F(n-2))$

End

**Table 2.** Tracking Algorithm

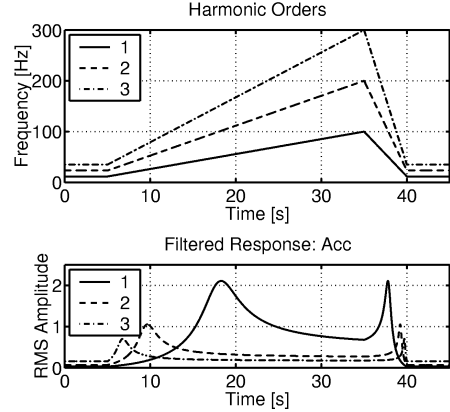


**Fig. 2.** Harmonic Orders of periodic signal. *Top graph:* the three curves show frequency profile of the three harmonic components in the driving force of the mechanical system. The harmonic orders decrease 3dB per octave. *Bottom graph:* RMS amplitudes of the acceleration response of the driving force. It shows that the relative amplitude of the harmonic components changes with the fundamental frequency; its start at the low frequency with the 3<sup>rd</sup> order dominating, then as the frequency increases first the 2<sup>nd</sup> order and then the 1<sup>st</sup> order dominates.

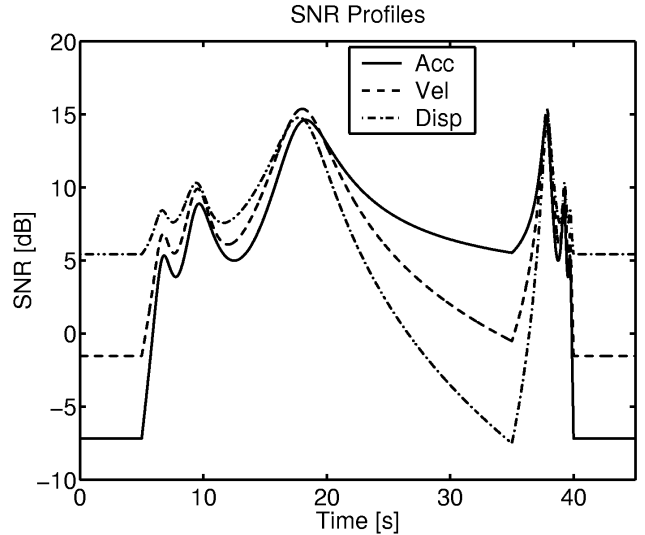


**Fig. 3.** Variation in SNR. This figure shows the non-stationary behaviour of the signal to noise ratio when the fundamental frequency and harmonic orders changes as shown in figure 2. The noise variance is set for each of the three responses, such that an overall SNR of 10 dB is achieved.

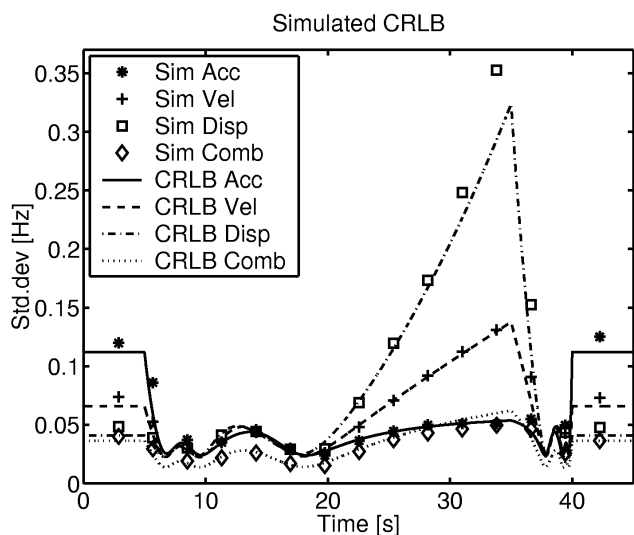


**Fig. 4.** Cramér Rao Lower Bounds. The estimated standard deviation,  $\sigma$ , of 100 Monte Carlo simulations of tracking fundamental frequency in the three different response signals are plotted here using symbols. With lines are shown the theoretical limits computed according to [4]. There is strong agreement between simulations and theory. It is noted that tracking on the joined posterior improves the estimate significantly.

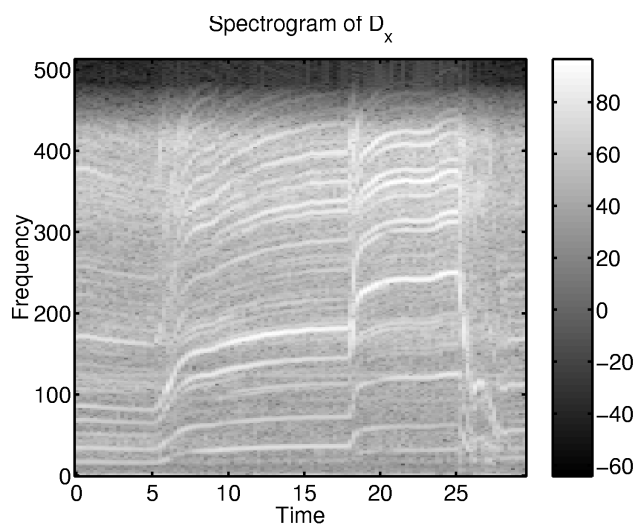


**Fig. 5.** Experimental Data. The spectrogram of the measured vibrations in the x direction is shown here. In the two other directions the spectrograms look similar (no shown).

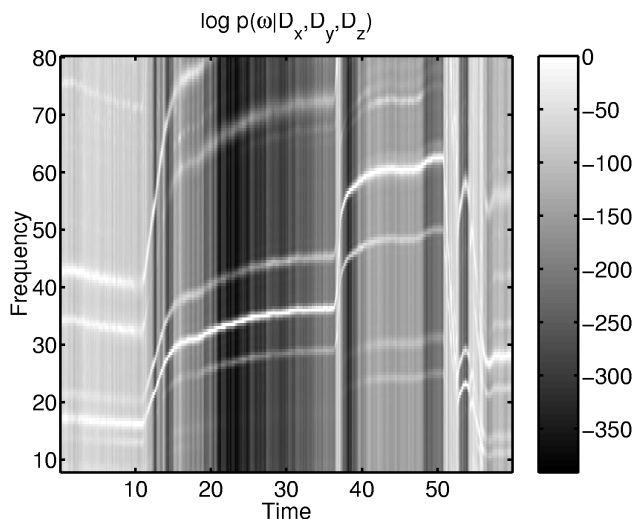


**Fig. 6.** Posterior distribution of combined signals. For each of the measured signals the posterior distribution for  $\omega_F$  is computed. Combining the three distribution results in the joined posterior distribution shown here conditioned on all three signals.

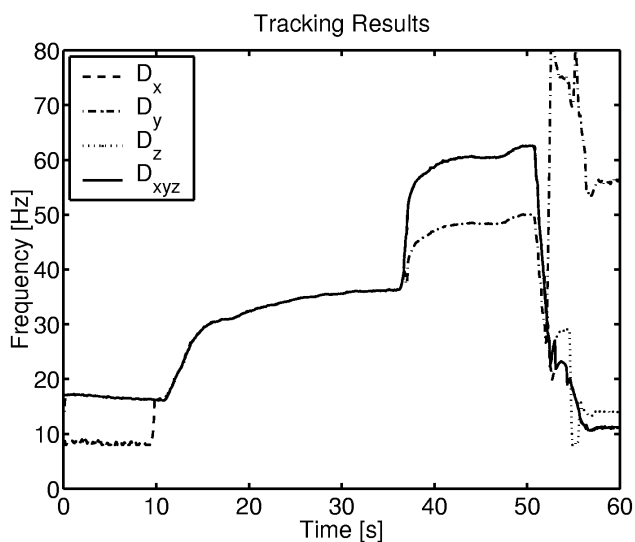


**Fig. 7.** Tracking Result. The four tracks shown here corresponds to tracking on the posterior conditioned on each of the source signals. The fourth track is from the combined posterior shown in figure 6. The deviations from the true track are summarized in table 1.